HHS Public Access

Author manuscript

Nat Med. Author manuscript; available in PMC 2017 August 09.

Published in final edited form as:

Nat Med. 2016 July ; 22(7): 812–821. doi:10.1038/nm.4103.

A Humanized Ossicle-niche Xenotransplantation Model Enables Improved Human Leukemic Engraftment

Andreas Reinisch[1], **Daniel Thomas**[1], **M. Ryan Corces**[1], **Xiaohua Zhang**[1], **Dita Gratzinger**[2], **Wan-Jen Hong**[1], **Katharina Schallmoser**[3,5], **Dirk Strunk**[4,5], and **Ravindra Majeti**[1]

[1]Department of Medicine, Division of Hematology, Cancer Institute, and Institute for Stem Cell Biology and Regenerative Medicine, Stanford, California, USA

[2]Department of Pathology, Stanford University School of Medicine, Stanford, California, USA

[3]Department of Blood Group Serology and Transfusion Medicine, Paracelsus Medical University, Salzburg, Austria

[4]Experimental and Clinical Cell Therapy Institute, Paracelsus Medical University, Salzburg, Austria

[5]Spinal Cord Injury & Tissue Regeneration Center Salzburg, Paracelsus Medical University, Salzburg, Austria

Abstract

Xenotransplantation models provide powerful tools for the investigation of human normal and malignant hematopoiesis. However, current models do not extensively recapitulate human bone marrow (BM) microenvironment components and exhibit limited engraftment of many human leukemias and other disorders. Here, we describe a xenotransplantation model bearing subcutaneous humanized ossicles with an accessible BM microenvironment formed by in situ differentiation of human BM-derived mesenchymal stromal cells. In these humanized ossicles, we observed robust engraftment of normal human hematopoietic stem and progenitor cells, and detected extensive engraftment of diverse primary acute myeloid leukemia samples at levels much greater than in unmanipulated mice. Direct intraossicle transplantation accelerated engraftment and resulted in substantially higher leukemia-initiating cell frequencies. We also observed robust engraftment of acute promyelocytic leukemia and myelofibrosis leading to the identification of leukemia-initiating cells in hematopoietic stem cells in myelofibrosis. This humanized ossicle xenotransplantation approach provides a novel system to model human hematologic disease.

Correspondence should be addressed to R.M. (rmajeti@stanford.edu).

Author Contributions. A.R. and R.M conceived and designed the project. A.R., D.T., M.R.C., W.H., and X.Z. performed the experimental work. A.R., D.T., M.R.C., and D.G. analyzed the data. K.S. and D.S. provided critical reagents. A.R. and R.M. wrote the manuscript. All authors discussed the results.

Introduction

Over the last several decades, a number of progressively more immunodeficient mice strains have been developed, and particularly with the development of NSG mice bearing a targeted deletion of the IL2-receptor gamma chain on the NOD-SCID background, engraftment of many human solid tumors and hematopoietic malignancies became feasible[1]. However, human hematopoietic cell engraftment often remained at low levels leading to the development of further strains with improved xenograft efficiency through overexpression or targeted insertion of human cytokines such as SCF, GM-CSF, IL-3, and TPO [2-5].

These mouse strains have been used extensively for the engraftment of human hematopoietic malignancies, particularly acute myeloid leukemia (AML) [6]. However, a large proportion of AML patient samples, in particular less aggressive subtypes such as core binding factor mutants and acute promyelocytic leukemia (APL), fail to engraft or do so at low levels that do not mimic human disease [7-9]. Additionally, many other hematopoietic neoplasms do not engraft in the currently available mouse strains, as transplantation of MDS, MPN, or multiple myeloma has met with very limited success [10-12], although in myelodysplastic syndrome (MDS), a recent study utilized a modified NSG engraftment assay through the co-transplantation of mesenchymal stromal cells (MSC) with HSC to identify MDS-initiating cells [13]. The reasons for this remain largely unclear, but likely include a dependence on species-specific environmental factors for homing, survival, and expansion that differ between mice and humans.

Hematopoiesis occurs primarily in the bone marrow (BM), where hematopoietic stem cells (HSC) are localized in specialized microenvironments known as BM niches. In these niches, HSC reside in close contact and bidirectional interaction with a complex network of cells including MSC, osteoblasts, adipocytes, vascular endothelial cells, and Schwann cells [14]. These niches not only provide sanctuary sites for HSC, but are also co-opted by leukemia cells in hematopoietic malignancies and can support LSC survival [15,16].

Recently, we have shown that immature mesenchymal stromal cells from human BM (BM-MSC) can recreate a functional hematopoietic microenvironment in NSG mice upon transplantation into ectopic sites through endochondral ossification to form a humanized ossicle [17]. We speculated that these ossicles contain a humanized microenvironment with the proper supply of human niche factors to facilitate superior engraftment and growth of normal and malignant human hematopoietic cells. Here, we show that this is indeed the case with human BM-MSC-derived ossicles exhibiting robust and superior engraftment of normal and malignant hematopoietic cells from acute leukemias and other hematopoietic disorders.

Results

Human hematopoietic stem and progenitor cells engraft robustly in human BM-MSC-derived ossicles

We sought to establish a xenotransplantation system for human normal and malignant hematopoietic cells through the generation of *in vivo* humanized BM niches in NSG mice [17] (Fig. 1a and see Supplementary Fig. 1a-f for a detailed protocol for humanized ossicle

formation). Subcutaneous transplantation of human BM-MSC admixed with extracellular matrix (up to four transplants per mouse) results in the robust formation of a humanized BM microenvironment within an ossicle after 8 – 10 weeks. Transplanted cells undergo endochondral ossification in situ and form a marrow cavity with concomitant invasion of mouse hematopoietic tissue, as indicated by a visible dark purple color change (Fig. 1a, and Supplementary Fig. 1e left panel). Daily administration of an anabolic dose of human parathyroid hormone (40 μg/kg) for 28 days after BM-MSC transplantation resulted in a significant increase in the size of the humanized ossicles (Supplementary Fig. 1f).[18,19] In order to confirm the human origin of ossicle bone and stromal niche elements, BM-MSC were transduced with lentivirus to stably express green fluorescent protein (GFP). Fluorescence microscopy demonstrated GFP^+ cells residing both within bone structures and within the marrow space of mature ossicles (Supplementary Fig. 1h). Once sufficient BM formation is detected, ossicle-bearing NSG mice are conditioned with sublethal irradiation and then transplanted with human normal or malignant hematopoietic cells either by intravenous injection, or by direct transcutaneous intraossicle injection (Fig. 1a, middle panel and Supplementary Fig. 1e,f). Because of their easily accessible subcutaneous location, human hematopoietic engraftment in the ossicles is monitored by serial aspiration and flow cytometry, with histologic assessments at the time the mice are sacrificed (Fig. 1a, right panel and Supplementary Fig. 1e,f).

We first investigated if the humanized niches could support human hematopoiesis by intravenous transplantation of human cord blood-derived $CD34^+$ hematopoietic stem and progenitor cells (HSPC), and in separate mice by direct intraossicle injection into one ossicle out of up to four per mouse. Independent of the transplantation route, human $CD45^+$ cells, including both $CD19^+$ lymphoid cells and $CD33^+$ myeloid cells, were detected in the humanized ossicles as early as four weeks post-transplantation (Supplementary Fig. 2a). Subsequent aspirates taken at 7 – 8 and 17 – 18 weeks post-transplantation revealed clear engraftment of human hematopoietic cells in all ossicles analyzed (Fig. 1b,c and Supplementary Fig. 2b). Human engraftment levels were higher in directly injected ossicles than in the BM of mice that received $CD34^+$ HSPC through intravenous transplantation (mean ± SD, 7 – 8 weeks: 86.0 ± 9.6% vs. 21.2 ± 26.3%; $P = 0.1$; 17 – 18 weeks: 90.1 ± 11.6% vs. 52.1 ± 26.6% $P = 0.06$) (Fig. 1c). Human engraftment levels were also significantly higher in directly injected ossicles compared to the non-injected ossicles and the BM of the same mice, whose engraftment was indicative of homing of HSPC from the injected ossicle to additional sites of hematopoietic niches (mean ± SD, 7 – 8 weeks: 86.0 ± 9.6% vs. 21.3 ± 26.5% vs. 23.5 ± 32.3%; $P < 0.001$; $P < 0.05$; 17 – 18 weeks: 90.1 ± 11.6% vs. 51.3 ± 28.0% vs. 39.9 ± 22.8% $P < 0.05$ for both comparisons) (Fig. 1c). Finally, intravenous transplantation of human HSPC showed a preference for engraftment of humanized niches at 17 – 18 weeks compared to mouse bone marrow (mean ± SD: 70.7 ± 27.3% vs. 52.1 ± 26.8% $P < 0.05$) (Fig. 1c).

At 17 – 18 weeks post-transplantation, we identified mature neutrophils, eosinophils, monocytes, mast cells, conventional and plasmacytoid dendritic cells as well as low levels of T cells (<4%), NK-cells (<0.2%), and variable numbers of cells committed to the megakaryocyte-lineage and nucleated erythroid precursors in the humanized ossicle niches. As expected, the majority of B-cells in the ossicles were immature B-cell precursors, and the

mature B cells were polyclonal for expression of immunoglobulin light chains kappa and lambda (Supplementary Fig. 2c-g).

Humanized ossicle niches retained and maintained human HSPC populations including hematopoietic stem cells (HSC), multipotent progenitors (MPP), lymphoid primed-multipotent progenitors (L-MPP), common myeloid progenitors (CMP), granulocyte-monocyte progenitors (GMP), and megakaryocyte-erythroid progenitors (MEP) (Supplementary Fig. 2h,i). Finally, the presence of functional self-renewing HSC within the ossicles was confirmed by successful engraftment of ossicle-derived cells in secondary recipients with and without established humanized ossicles (Supplementary Fig. 2j).

Primary acute leukemia cells engraft robustly in human BM-MSC-derived ossicles

Next, we investigated the engraftment of primary human acute leukemia cells, both AML and ALL, through direct intraossicle injection (see Supplementary Table 1 and 2 for patient sample information). In the first case, individual ossicles were directly injected with 10,000 AML blasts, and leukemia engraftment in the transplanted ossicle, as well as the corresponding mouse BM, was investigated. Transplanted ossicles exhibited a very high level of leukemic engraftment at 12 weeks post-transplantation with >95% $CD45^{low}CD33^{+}$ leukemic blasts in all ossicles, and leukemic egress from the humanized ossicle niches led to a high burden of leukemia in the mouse BM (Fig. 1d,e). Intraossicle transplantation of a diverse cohort of AML samples demonstrated leukemia engraftment in 13 out of 15 samples, with 12/13 achieving >95% human leukemic chimerism in the transplanted ossicles (Table 1). Moreover, intravenous transplantation of ossicle-bearing mice led to >80% leukemic engraftment in the ossicles with 4 out 4 AML samples (Table 1). In addition to AML, both patient-derived B-cell acute lymphoblastic leukemia (B-ALL) and T-cell acute lymphoblastic leukemia (T-ALL) engrafted at high levels in the ossicles after 8 – 11 weeks, and eventually completely took over the mouse BM with $CD45^{+}CD19^{+}$ or $CD45^{+}CD3^{+}$ cells, respectively (Fig. 1d,e).

Primary AML blasts preferentially engraft humanized ossicle niches compared to mouse bone marrow

The high frequency and level of engraftment upon direct intraossicle injection suggested that the humanized ossicle niches were superior to mouse BM for the engraftment of human AML. In order to make direct comparisons, we identified 4 samples that engrafted poorly upon intravenous transplantation into unmanipulated NSG mice, with either low chimerism or very delayed kinetics (Table 1). 1×10^6 primary AML blasts from each of these samples were either (i) directly injected in one ossicle per mouse, (ii) transplanted intravenously into mice bearing up to four ossicles, or (iii) transplanted intravenously into unmanipulated NSG mice (Fig. 2a). The kinetics and burden of $CD45^{+}CD33^{+}$ leukemia engraftment were evaluated by flow cytometry in all ossicles and the mouse BM every 4 – 6 weeks starting at eight weeks post-transplantation (Fig. 2a,b and Supplementary Fig. 3,4). At eight weeks post-transplantation, a high leukemia burden was detected in directly injected humanized ossicles compared to almost undetectable engraftment in the unmanipulated NSG mice BM (mean ± SD, 89.6 ± 10.4% vs. 2.1 ± 4.6%; $P < 0.0001$) (Fig. 2b). Leukemia cells initially engrafted in humanized ossicles after direct injection preferentially disseminated to non-

transplanted ossicles compared to the BM of the same mouse over the course of 8-24 weeks post-transplantation (mean ± SD at 8 weeks: 22.1 ± 26.9% vs. 4.6 ± 3.9%; $P = 0.09$, 12-13 weeks, 74.1 ± 30.4% vs. 30.37 ± 40.9%; $P < 0.05$, 18-24 weeks, 88.5 ± 17.7% vs. 60.8 ± 33.6%; $P < 0.05$ (Fig. 2b). Histological analysis 8 weeks post-transplantation recapitulated the flow cytometry results, demonstrating very high human $CD45^+$ leukemia burden in the directly injected ossicles, and already revealed low level engraftment and repopulation in the non-transplanted ossicles of the same mice (Fig. 2c). Note that in the non-transplanted ossicles, human leukemia cells were almost exclusively localized to the endosteal paratrabecular regions previously demonstrated to be preferred niches for both normal HSC and AML LSC [15,20].

A similar preferential engraftment of the humanized niches was observed in intravenously injected mice bearing ossicles. At 8 weeks post-transplantation, all ossicles were engrafted with human leukemia cells, whereas the mouse BM showed significantly less engraftment, and in some cases even a complete absence of human cells (mean ± SD, 8 weeks, 14.4 ± 19.1% vs. 2.5 ± 1.8%, $P < 0.01$) (Fig. 2a,b and Supplementary Fig. 3,4). Subsequent analysis performed at 12 – 13 weeks and 18 – 24 weeks post-transplantation demonstrated a continued statistically significant increased engraftment in the ossicles compared to mouse BM, with near complete replacement of mouse hematopoiesis in most ossicles by 12 – 13 weeks (Fig. 2b). By 18 – 24 weeks, leukemia burden in the BM of mice without humanized ossicles was significantly lower than engraftment in the ossicles after intravenous injection (mean ± SD, 18 – 24 weeks: 13.4 ± 20.1% vs 89.5 ± 14.1%; $P < 0.0001$). Interestingly, the presence of humanized ossicles eventually increased the engraftment of human leukemia in the BM of the same mouse compared to unmanipulated mice (mean ± SD, 18 – 24 weeks: 48.0 ± 33.2% vs. 13.4 ± 20.1%; $P < 0.001$). As expected, histological analysis demonstrated effacement of the ossicle marrow cavity with human AML cells that showed typical morphological features of myeloid blasts (Supplementary Fig. 5a,b), and molecular analysis identified leukemia-associated mutations and/or translocations in the engrafted cells (Supplementary Fig. 5c and Supplementary Table 3).

With these 4 AML samples, the absolute number of leukemia cells recoverable from humanized ossicle niches in a single mouse (four ossicles per mouse) was significantly higher than the cells that could be isolated from the corresponding mouse BM. We recovered an average of $5.8 \pm 1.5 \times 10^7$ (mean ± SD, SU306: $5.4 \pm 0.4 \times 10^7$; SU480: $5.2 \pm 0.9 \times 10^7$; SU532: $5.8 \pm 0.1 \times 10^7$; SU582: $5.0 \pm 1.1 \times 10^7$) human leukemia cells combined from all 4 explanted ossicles of mice transplanted with samples SU306, SU480, SU532 and SU582, whereas absolute leukemia cell counts recoverable from total mouse BM were significantly lower with an average of $1.6 \pm 2.3 \times 10^7$ human leukemia cells and varied depending on engraftment levels ($P < 0.0001$ for all samples combined, unpaired t-test, SU306: $8.9 \pm 1.5 \times 10^6$; SU480: $3.7 \pm 2.7 \times 10^7$; SU532: $1.4 \pm 2.6 \times 10^7$; SU582: $5.9 \pm 4.8 \times 10^6$, Supplementary Fig. 5d).

AML blasts engrafted in humanized ossicle niches recapitulate the subclonal architecture of the original blasts

Recent work has suggested that conventional NSG mouse xenograft assays do not fully recapitulate the clonal heterogeneity of patient samples, resulting in engrafting subclones that may be distinct from the dominant founding or relapse clone, presumably due to selective pressure imparted by the mouse BM microenvironment [21]. We investigated the clonal composition of human AML cells engrafted in the humanized ossicle niches through targeted re-sequencing of known leukemia mutations in four of our engrafted normal karyotype cases. For all samples analyzed (SU306, SU480, SU532, and SU582), we detected the same variants (SNPs and Indels) in the primary patient samples and the ossicle-engrafted leukemia cells at similar variant allele frequencies (Supplementary Fig. 5c). Interestingly, AML blasts transplanted by direct intraossicle injection most closely recapitulated the clonal heterogeneity of the original patient blasts, whereas engrafted cells in the mouse BM after intravenous transplantation tended to show variable variant allele frequencies. For example, in sample SU532, a canonical mutation in *NPM1* was detected in the original blasts and the cells from the engrafted ossicles at similar levels; however, a subclone without this *NPM1* mutation engrafted the mouse BM of intravenously transplanted animals, demonstrating that the ossicle model was able engraft the subclones present in this case.

Humanized ossicle niche transplantation reveals an increased leukemia-initiating cell frequency in AML

Original studies using limiting dilution xenograft assays suggested that leukemia-initiating cells (LIC) in AML were rare, comprising 1 : 10,000 or fewer cells [22,23]. In order to determine if transplantation of AML cells into a humanized microenvironment can facilitate increased engraftment and frequency of LIC, we conducted limiting dilution assays with two AML samples using both direct intraossicle transplantation and direct intrafemoral transplantation in unmanipulated NSG mice. Cells from case SU028 demonstrated engraftment in the ossicles from all mice transplanted with as few as 100 cells, while no engraftment was detected by intrafemoral transplantation with 100 cells (Fig. 3a,b). In fact, we observed leukemic engraftment from transplantation of a single SU028 $CD34^{+}CD38^{-}$ leukemic blast in a humanized ossicle (Fig. 3c), resulting in an approximately 27-fold increase in the frequency of LIC to 1:20 cells (Fig. 3b and Supplementary Table 44). In the case of SU048, complete engraftment (>95%) was detected in the injected ossicles from as few as 500 cells, compared to very low engraftment (<1%) in mice transplanted intrafemorally with 1,000 cells, resulting in a 10-fold increase in LIC frequency to 1:271 cells (Fig. 3d,e and Supplementary Table 4)

Humanized Ossicle Niches Facilitate Robust Engraftment of Acute Promyelocytic Leukemia Cells which Derive from Lineage-Committed Leukemia-Initiating Cells

Transplantation of human acute promyelocytic leukemia (APL) into immunocompromised mice has so far been of limited success with low to no detectable engraftment [9,23]. Since humanized ossicle niches show superior engraftment of non-APL AML samples, we investigated the engraftment of primary human APL cells by direct intraossicle injection. 0.9

– 1.4×10^6 mononuclear cells from primary APL samples were transplanted into humanized ossicles and engraftment was monitored over time. As early as 6 – 8 weeks post-transplantation, injected ossicles developed detectable levels of $CD45^+CD33^+$ leukemia cells (mean ± SD, SU589: 41.2 ± 27.4%; SU490: 21.5 ± 8.2%; SU748: 5.1 ± 7.1%; SU718: 0.3 ± 0.5%) (Fig. 4a,b and Supplementary Fig. 6a-c). Although in 2/4 samples (SU490 and SU589) the transplanted cells initially gave rise to combined lymphoid and myeloid cells at six weeks post-transplantation, further propagation of APL blasts resulted in an almost complete engraftment of the ossicle marrow with leukemia cells at 12 – 24 weeks (mean ± SD, SU589: 94.1 ± 8.5%; SU490: 90.5 ± 5.6%; SU748: 78.9 ± 32.3%; SU718: 97.2 ± 1.3%) (Fig. 4a,b and Supplementary Fig. 6a-c), but much lower engraftment of leukemic cells was detected in the mouse BM (Fig. 4a,b). Myeloid cells isolated from the engrafted ossicles were confirmed to harbor the characteristic PML-RARA translocation by fluorescence in situ hybridization (FISH) (Fig. 4c and Supplementary Fig. 6a-c). Gross examination of the explanted ossicles revealed formation of subcutaneous granulocytic sarcomas or chloromas, as indicated by their yellow-green appearance, and histological analysis of engrafted ossicles identified densely packed immature blasts morphologically resembling promyelocytes (Fig. 4d). May-Gruenwald Giemsa staining confirmed the presence of azurophilic granules or characteristic cerebriform, bi-lobed nuclei pathognomonic for the microgranular variant of APL (Fig. 4d).

The successful engraftment of primary human APL cells provided the opportunity to investigate leukemia-initiating cells (LIC) in this disease, which has been a point of controversy in the field.[24] First, we isolated a $CD34^+CD38^-CD45RA^-$ fraction that normally contains HSC and MPP from primary APL samples and compared engraftment of these cells to bulk APL cells in humanized ossicle niches by direct intraossicle injection. In contrast to bulk cells that transiently (6 – 8 weeks post-transplantation) gave rise to combined lymphoid and myeloid cells before being replaced by 100% myeloid cells harboring the PML-RARA translocation (Figure 4a), transplanted HSC/MPP produced normal B-cells and myeloid cells lacking the PML-RARA translocation for up to 24 weeks (Supplementary Fig. 6d,e), suggesting that LIC in APL reside in a cell that is downstream of HSC/MPP. This idea was further supported by FISH analysis of subpopulations isolated from several primary APL samples, which demonstrated that HSC/MPP, CMP, and MEP lacked the PML-RARA translocation in all samples analyzed (Supplementary Table 5). However, this translocation was detected in aberrant $CD34^{lo/-}$ GMP-like cells, which did give rise to PML-RARA-positive APL in transplanted ossicles (Supplementary Fig. 6e). Thus, leukemia-initiating cells in APL do not reside in HSC/MPP, and likely reside in a lineage-committed progenitor.

Humanized ossicle niches facilitate robust engraftment of myelofibrosis which derives from leukemia-initiating cells in the HSC compartment

Myelofibrosis (MF) is a myeloproliferative neoplasm (MPN) commonly associated with *JAK2*^{V617F} and calreticulin (*CALR*) mutations [25-28] that has shown only limited engraftment with transplantation of large numbers of patient-derived $CD34^+$ cells in conventional xenograft models [29-31]. We examined the ability of humanized ossicles to facilitate the engraftment of MF (see Supplementary Table 6 for patient sample information) through the direct intraossicle injection of FACS-purified $CD34^+$ cells. Transplantation of a maximum of

50,000 $CD34^+$ cells resulted in robust engraftment (up to >95%) of human hematopoietic cells for up to 19 weeks post-transplantation (Fig. 5a,b). Interestingly, the engrafted cells were mainly comprised of $CD33^+$ myeloid cells, with minimal to absent reconstitution of B cells, which are the predominant population in mice engrafted with normal human $CD34^+$ cells (Fig. 5c). Allele-specific quantitative real-time PCR demonstrated that engrafted human $CD45^+CD33^+$ myeloid cells at 8 – 19 weeks post-transplantation harbored the $JAK2^{V617}$ mutation in 4/4 samples, indicating they were derived from the transplanted MF cells (Fig. 5d). The $JAK2^{V617F}$ mutant allele burden in the engrafted cells was nearly identical to the allele burden in the HSPC and myeloid cells isolated from the primary sample both in a homozygous (SU094.D, SU415) or heterozygous (SU180, SU482) manner (Supplementary Fig. 7a). For sample SU239B harboring a Type1 *CALR* mutation (52bp deletion), we confirmed the presence of the mutation in the engrafted myeloid cells by Sanger sequencing (Supplementary Fig. 7d). Consistent with engraftment of myelofibrosis-initiating cells, histological analysis identified an increase in reticulin fibers within the engrafted humanized ossicles (Fig. 5e).

The successful engraftment of primary human MF cells provided the opportunity to investigate leukemia-initiating cells in this disease, which have long been hypothesized to reside in the HSC compartment [32]. We first fractionated $CD34^+$ cells from MF samples into $CD34^+CD38^+$ and $CD34^+CD38^{lo/-}$ subfractions and transplanted each directly into multiple humanized ossicles ($n = 4 – 7$ per sample). In all three samples tested, engraftment of human cells was exclusively observed in ossicles transplanted with $CD34^+CD38^{-/lo}$ cells ($n = 19$ ossicles) with no engraftment from the $CD34^+CD38^+$ cells ($n = 12$ ossicles), although higher numbers of these cells were transplanted (Supplementary Table 7).

We further fractionated the $CD34^+CD38^{low/-}$ cells from sample SU482 and SU239.B into HSC and MPP[33], and tested their engraftment potential through direct intraossicle injection. As a negative control, we also transplanted CMP from the $CD34^+CD38^+$ fraction (Supplementary Table 5). Eight weeks post-transplantation, human $CD45^+$ cells were only detectable in ossicles transplanted with HSC, but not MPP or CMP (Fig. 5f and Supplementary Fig. 7b), and the engrafted myeloid cells harbored the $JAK2^{V617F}$ mutation or the Type I *CALR* mutation (52 bp deletion) (Supplementary Fig. 7c,d). These results formally demonstrate that MF-disease-initiating cells reside exclusively in the HSC compartment.

Discussion

Here, we describe a xenotransplantation system that greatly improves upon existing models through the in situ subcutaneous generation of human BM-MSC-derived ossicles, forming a humanized BM microenvironment that more effectively supports normal and malignant hematopoiesis. Original xenotransplantation studies suggested AML LIC/LSC were rare cells, on the order of 1 : 10,000 – 100,000 enriched in the $CD34^+CD38^-$ fraction of leukemic blasts [22,23]. More recent studies suggested that LIC/LSC are more frequent and can be found in additional immunophenotypically defined subpopulations [7,34,35]. Here, we provide evidence that with a humanized niche, the frequency of LIC is substantially higher than that

determined in the NSG mouse BM with the same sample, suggesting that AML LIC frequency is critically dependent on leukemia cell-niche interactions.

The identification of disease-initiating cells in acute promyelocytic leukemia has been hampered by the lack of a xenotransplantation model. In APL, the nature of the hematopoietic cell that is the target of the disease-causing chromosomal translocation is a matter of debate[24] with *in vitro* studies implicating immature compartments able to produce myeloid and erythroid output [36], and alternative reports supporting APL arises from committed myeloid progenitors.[37-39] Here, we report successful fulminant engraftment of PML-RARA-positive human APL cells in humanized ossicles, and identification of APL-initiating cells in an aberrant $CD34^{-/lo}$ GMP-like population. This further supports the notion that APL is a disease arising from committed myeloid cells and most likely does not involve immature hematopoietic stem and progenitor cells. Our experiments still leave open the possibility that $CD34^{-}$ cells, which are the majority of cells in most APL cases, also contain disease-initiating cells. These results are consistent with mouse models that drive expression of PML-RARA from a myeloid lineage-restricted promoter resulting in an APL-like disease [40,41]. The absence of PML-RARA translocation in human HSC obtained from APL patient samples is surprising given that PML-RARA on its own induced myeloid commitment rather than self-renewal in hematopoietic progenitors such as GMP [42]. In contrast to a recently published report demonstrating establishment of APL from transduced cord blood-derived CMP, we did not identify PML-RARA fusion events in FACS-purified CMP from primary patient samples [43]. How PML-RARA initiates a self-renewal program in human progenitors to cause APL is an important question for further studies of APL pathogenesis.

Similar to APL, our humanized ossicle model facilitates robust engraftment of primary human MF cells, which has only been of limited success with peripheral blood derived cells with conventional NSG models.[31,44] Unlike studies of AML, where disease-initiating cells arise from progenitors [35], we show here that myelofibrosis-initiating cells reside in the HSC compartment, as transplantation of these cells, but not MPP or CMP, results in engraftment of $JAK2^{V617F}$ or *CALR*-mutant cells. Notably, progeny from these MF HSC exhibited a pronounced skewing towards the myeloid lineage, suggesting that the $JAK2^{V617F}$ and *CALR* mutations drive a differentiation program blocking lymphoid development in favor of myeloid cells.

Recently, several newly developed xenotransplantation models have been reported for improved engraftment of human hematopoietic cells including modified NSG strains with overexpression or knock-in of human cytokines [2,4,5,45,46], co-transplantation of hematopoietic cells with mesenchymal stromal cells [13], and transplantation of engineered bio-scaffolds designed to resemble human BM niches [47]. While each of these approaches has advantages compared to conventional NSG mouse models, they have not demonstrated the rapid and high leukemic engraftment observed with our humanized ossicle niche model, where direct intraossicle injection resulted in >95% leukemic chimerism in nearly all engrafting leukemia samples tested (Table 1). These observations indicate that our approach more faithfully models human disease providing a superior system for further investigation

into human leukemia pathogenesis, leukemia cell-niche interactions, and responses to therapeutics.

Online Methods

Primary human samples

AML, ALL, MF, and cord blood samples were obtained according to the Administrative Panel on Human Subjects Research Institutional Review Board (IRB)-approved protocols (Stanford IRB no. 18329, no. 6453, and no. 5637) after informed consent. Cord blood was collected after written informed consent by the mother obtained prior to delivery of full-term pregnancies at the Lucile Packard Children's Hospital according to IRB-approved protocols (Stanford IRB no. 5637) or purchased from the New York Blood Center (NYBC). All cord blood samples were processed within 24 hours after delivery and used fresh. All of the primary AML samples used in this study were tested for mutations in FLT3, NPM1, IDH1, and IDH2 by the Stanford Anatomic Pathology and Clinical Laboratories.

Animal Care

All mouse experiments were conducted in accordance with a protocol approved by the Institutional Animal Care and Use Committee (Stanford Administrative Panel on Laboratory Animal Care no. 22264) and in adherence to the US National Institutes of Health's Guide for the Care and Use of Laboratory Animals.[48]

BM-MSC culture and immunophenotyping

Human BM samples were obtained according to Medical University of Graz Ethikkommission (Institutional Review Board-approved protocol, MUG Graz IRB no. 19-252). BM-MSC were isolated and expanded as previously described.[17,49,50] Age of healthy BM donors ranged from 21 – 45 years. Briefly, BM-MNCs were washed out from BM collection filters by flushing the filters with pre-warmed PBS. Total washouts were spun down (300 g, 7min, 4°C) and resuspended in pre-warmed α-modified minimum essential medium (α-MEM; Sigma-Aldrich, St. Louis, MO) containing 10% pooled human platelet lysate (pHPL) and seeded into culture vessels. Non-adherent cells were removed by rinsing the plastic with PBS and adherent cells were further expanded. Emerging colonies (CFU-F) were passaged for further cell propagation. For large-scale expansions prior to transplantation into NSG mice, BM-MSC were cultured in four-layered cell factories (CF-4, Thermo Fisher, Nunc, Pittsburg, PA) with half-weekly medium changes until cells reached confluence. At the end of passage 1 (p1), BM-MSC were profiled for expression of consensus MSC surface markers.[51] Briefly, trypsinized cells were blocked with sheep serum (10% v/v) and thereafter stained with following monoclonal antibodies for 30 min, 4°C in the dark: CD90-BUV395 (dilution 1:5; clone: 5E10), CD73-PE (dilution 1:33; clone: AD2), CD29-APC (dilution 1:100; clone: MAR4), CD45-APC (dilution 1:25; clone: 2D1), CD14-PE (dilution 1:25; clone: MφP9), CD34-PE-Cy7 (dilution 1:50; clone: 8G12), CD19-BUV395 (dilution 1:25; clone; SJ25C1, all BD Biosciences, San Jose, CA), CD105-eF450 (dilution 1:25; clone: SN6), HLA-DR-eF450 (dilution 1:50; clone: L243, both ebioscience, San Diego, CA) and corresponding isotype controls. At least 10,000 viable cells (FVD eF520; dilution 1:100; ebiosience) were acquired and analyzed using a BD Fortessa flow

cytometer. Raw FCS files were analyzed using FlowJo software (Treestar, Ashland, OR) and histograms were generated.

Humanized ossicle-niche formation

Confluent BM-MSC were harvested using trypsin-based dissociation reagent (TrypLE Express, Thermo Fisher, Gibco). 2×10^6 MSC were pelleted and resuspended in 60 μl of pure filter pHPL and admixed with 240 μL of matrigel-equivalent matrix (Angiogenesis assay kit, Millipore, Billerica, MA). Total volume of 300 μl matrix-cell mixtures was injected subcutaneously to generate humanized ossicle niches (up to four injections per mouse) into the flanks of 6 – 12 week old immunodeficient NOD.Cg-Prkdc^{scid} Il2rg^{tm1Wjl}/SzJ (NSG) mice (Jackson Laboratory, Bar Harbor, ME). Starting at day +3 – 7, mice received daily subcutaneous injections of human parathyroid hormone (PTH [1-34]; R&D Systems, Minneapolis, MN; 40 μg/kg body weight; dorsal neck fold) for 28 consecutive days to further promote bone marrow niche formation, as previously described.[18,19] Eight – 10 weeks post BM-MSC application the site of injection was shaved and transplants were evaluated for bone and marrow formation by palpation and by visual inspection (development of a purple hue is indicative of bone marrow niche formation).

NSG hematopoietic xenotransplantation

Untreated female NSG mice (age: 6 – 8 weeks) or mice with established humanized ossicle-niches were conditioned with 200 rad of irradiation 12 – 24 hours prior to transplantation (Faxitron, X-ray irradiation). Cells were either transplanted (i) intravenously (150 μl, lateral tail vein) into untreated mice, (ii) intravenously into mice bearing four humanized ossicle-niches, or (iii) by direct intraossicle injection into one or up to four humanized ossicle-niches per mouse (20 μl). For transplantation 2-5 mice were randomly assigned to the different groups, as described above.

HSPC were enriched from freshly processed cord blood samples by magnetic separation using CD34 microbeads (Miltenyi Biotec, San Diego, CA) following the manufacturer's instructions. $1 \times 10^4 – 1 \times 10^5$ purified CD34$^+$ HSPC (purity >95%) were transplanted. Freshly thawed primary AML samples were either subjected to T cell depletion using anti-CD3 magnetic beads (Robosep, Stem Cell Technologies, Vancouver, Canada) or FACS-purified (Aria II, BD Biosciences) based on side scatter properties and low CD45 expression on AML blasts. $1 \times 10^6 – 5 \times 10^6$ T cell-depleted or FACS-purified AML cells were transplanted. Freshly thawed myelofibrosis samples were FACS-sorted using a previously established panel including anti-human lineage markers CD2 (clone: RPA-2.10), CD3 (clone: HIT3a), CD4 (clone: RPA-T4), CD7 (clone: M-T701), CD8 (clone: RPA-T8), CD11b (clone: ICRF44), CD14 (clone: MφP9), CD16 (clone: 3G8), CD19 (clone: H1B9), CD20 (clone: clone: 2H7), CD56 (clone: B159, all PE-Cy5; all dilution 1:50), GPA-PE-Cy5 (dilution: 1:100; clone: GA-R2, all BD). Additionally, the following antibodies were used: CD38-PE-Cy7 (dilution 1:50; clone: HB7), CD90-FITC (dilution 1:25; clone: 5E10), CD123-PE (dilution 1:10; clone: 7G3), CD34-APC (dilution 1:25; clone: 8G12, all BD), CD10-APC-Cy7 (dilution 1:10; clone: HI10a), and CD45RA-BV605 (dilution 1:20; clone: HI100, both Biolegend, San Diego, CA). Double-sorted, live, Propidium-Iodide^{neg} (PI, Thermo Fisher, final concentration: 1 μg/ml) HSPC subpopulations (purity >95%) were

transplanted. For limiting dilution analysis, cells were additionally applied intrafemorally through direct injection into the mouse femur (20 μl). For single cell transplantation, $Lin^-CD34^+CD38^-$ cells were sorted into single wells of Terasaki plates (Nunc MiniTrays, Thermo Fisher) prefilled with 10 μL IMDM 10% FBS as previously described [52] using FACS AriaII. Efficiency of single cell sorting was evaluated by microscopic inspection of an additional sorted plate. Cells were transferred into 31G insulin needles and transplanted directly into humanized ossicle-niches.

For secondary transplantation, 7,500 FACS-purified CD34+ cells isolated from engrafted ossicles were transplanted into irradiated NSG mice with and without pre-established ossicle niches.

Assessment of human engraftment

Engraftment of human cells within humanized BM-niches or mouse BM was assessed unblinded. BM aspirates were taken directly from engrafted humanized niches or the corresponding mouse BM using 27.5 G syringes. In case of post mortem analysis, explanted ossicles were crushed using mortar and pestle and femur/tibia were flushed. To remove contaminating red blood cells ACK lysis was performed (RBC lysis buffer, ebioscience), thereafter cells were blocked for nonspecific antibody binding (10% vol/vol sheep serum, 20 min, 4 °C) and stained (30 min, 4 °C, dark) with fluorochrome-conjugated monoclonal antibodies binding human CD45-V450 (dilution 1:25; clone: HI30), CD19-APC (dilution 1:25; clone: HIB19), CD3-APC-Cy7 (dilution 1:50; clone: SK7), CD33-PE (dilution 1:25; clone: WM53), mouse CD45.1-PE-Cy5 (dilution: 1:100; clone: 30-F11, all BD) and HLA-ABC-FITC (dilution 1:50; clone: W6/32, ebioscience). Normal multi-lineage engraftment was defined by the presence of myeloid cells ($CD33^+$) and B-cells ($CD19^+$) among engrafted human $CD45^+$ $HLA\text{-}ABC^+$ cells. AML engraftment was defined by the presence of a $CD45^+CD33^+$ population and absence of other hematopoietic cells. Mice engrafted with cord blood were additionally stained with antibodies to CD14-PE (dilution: 1:100; clone: MφP9), CD15-FITC (dilution 1:50; clone: MMA), CD117-APC (dilution 1:25; clone: YB5.B8), CD11c-V450 (dilution 1:25; clone: B-Ly6), CD11b-PE-Cy7 (dilution 1:25; clone: ICRF44), CD123-PE (dilution 1:10; clone: 7G3), and kappa-light chain-FITC (dilution 1:50; clone: TB28-2) and, lambda-light chain-PE (dilution 1:50; clone: 1-155-2), CD41-APC (dilution 1:25; clone: HIP8) and CD235a-PE (dilution 1:100; clone: GA-R2 all BD), HLA-DR-eF450 (dilution 1:25; clone: LN3), FcER1-FITC (dilution 1:25; clone: AER-37), mCD45-APC-Cy7 (dilution 1:25; clone: A20, all ebioscience), CD1c (BDCA-1)-APC (dilution 1:10; clone: AD5-8E7), CD303 (BDCA-2)-APC (dilution 1:10; clone: AC144, both Miltenyi) and CD56-APC-Cy7 (dilution 1:25; clone: 5.1H11, Biolegend) to further assess myeloid, lymphoid, erythroid, and megakaryocyte lineage. In particular CD41a and CD235a antibodies specifically recognize human but not mouse antigens.

JAK2 genotyping

Allele-specific *JAK2* genotyping assays were performed as described previously.[53] Briefly, engrafted human B cells ($huCD45^+CD19^+$) and myeloid cells ($huCD45^+CD33^+$) were sorted on an Aria II flow cytometer (BD) for analysis. Genomic DNA was isolated using QIAmp DNA mini kit (Quiagen, Valencia, CA), amplified (14 cycles, using allele specific primers),

and thereafter subjected to qPCR using TaqMan SNP genotyping assay (Applied Biosystems, Thermo Fisher) according to manufacturer's instructions.

CALR mutation screening

Genomic DNA was isolated from FACS sorted $CD33^+$ engrafted myeloid cells and 150 ng was amplified (25 cycles) using PCR SuperMix High Fidelity (Invitrogen) Forward primer: 5′-TGTAAAACGACGGCCAGTAAGCAAGGGCTATCGGGTAT-3′, Reverse primer: 5′-CAGGAAACAGCTATGACCAACCAAAATCCACCCCAAAT-3′. Final primer concentration was 200 nM, annealing temperature and extension temperature were 56°C and 68°C, respectively. PCR products were purified with QIAquick PCR Purification Kit (Qiagen), and Sanger Sequencing was performed to determine specific indels. Sequencing primer: 5′-TGTAAAACGACGGCCAGT-3′

AML Sample Genotyping

AML samples engrafted in ossicles or corresponding mouse BM, as well as sorted $CD45^{dim}$ AML blasts and $CD3^+$ T-cells from AML patients, were genotyped by customized hybrid capture sequencing (SeqCap EZ Choice kit, Roche/Nimblege, Madison, WI) targeting 130 of the most frequently mutated genes in AML. The native samples (prior to xenotransplantation) were genotyped by whole exome sequencing (SeqCap EZ Exome SR kit v3.0, Roche/Nimblegen) as previously described [54]. All kits were used following manufacturer's instructions (Roche/Nimblegen). Illumina HiSeq 2000, HiSeq 2500, or NextSeq 500 instruments were used for sequencing.

Morphological analysis

FACS-sorted purified cells were spun onto Poly-L-lysine pre-coated slides (Shandon Cytospin® centrifuge, Thermo Electric). May-Grunwald-Giemsa staining was performed using standard procedures. Light microscopy images were taken on a Leica DM5500B microscope equipped with Leica Application Suite V4 software (Leica Microsystems, Buffalo Grove, IL).

Fluorescence in situ hybridization

Engrafted FACS-purified myeloid cells were FACS-sorted, treated with hypotonic solution (0.075M KCl, 15 min, 37 °C) and fixed with methanol and glacial acid (3 : 1, 30 min, RT) before spinning onto Poly-L-lysine pre-coated slides. Interphase FISH analysis for t(15;17) or inv16 was performed using a PML-RARA Dual Color, Dual Fusion Translocation Probe or CBFB break apart Probe (Abbott, Des Plaines, IL), Briefly, ethanol-dehydrated specimens, pretreated per the manufacturer's instructions, were denatured (80°C, 8 min) and hybridized (37 °C, 20 hours) using a Vysis®HYBrite instrument. Slides were washed with 0.4 × SSC (0.3% NP-40, pH 7.0, 73 °C, 2 min) and with 2 × SSC (pH 7.0, RT, 2 min) counterstained with DAPI and analyzed on a Olympus BX51 microscope equipped with an 100 × oil immersion objective, appropriate fluorescent filters and CytoVision® imaging software (Leica Microsystems). Whenever possible, 200 nuclei were analyzed per condition.

Histological studies

Immunohistochemistry—Tissues were fixed with 4% paraformaldehyde immediately after explantation. Hematoxylin-eosin (H/E) staining and IHC staining were performed using standard protocols [17]. For IHC staining, temperature-based antigen retrieval was performed (70 °C, 160 W, 40 min) followed by a descending alcohol series. Endogenous peroxidases were blocked with hydrogen peroxide (10 min) and nonspecific antibody binding with Ultra V Block (5 min; Thermo Fisher) followed by mouse-on-mouse blocking (MOM, 1 hour; Vector Laboratories, Burlingame, CA) and serum-free protein block (30 min; Dako, Glostrup, Denmark). Slides were incubated (30 min, RT) with unconjugated monoclonal mouse anti-human antibodies against CD45 (dilution 1:1000; clone: 2B11, Dako) and developed with ultravision LP large volume detection system horseradish peroxidase (HRP) polymer (Thermo Fisher) and diaminobenzidine (DAB) according to manufacturer's instructions. Cells were counterstained (10 sec) with hematoxylin.

Reticulin staining—Tissue sections were deparaffinized and re-hydrated with distilled water. Slides were oxidized in 0.5% potassium permanganate (5 min) before being rinsed in running tap water (2 min). 2% potassium metabisulfite was applied (2 min), samples were again rinsed in running tap water (2 min), and then sensitized in 2% ferric ammonium sulfate (10 min). After another rigorous rinse in distilled water (1 min), ammoniacal silver nitrate solution was applied (5 min) and thereafter rinsed quickly in 3 changes of distilled water (30 sec each). Slides were transferred to 20% un-buffered formalin rinsed in running tap water (2 min) and toned in 0.2% gold chloride (10 min). Another rinse in running tap water 1 min was followed by incubation with 2% potassium metabisulfite (2 min). After rinsing in running tap water (1 min) excess silver in 2% sodium thiosulfate was removed (2 min). Eventually slides were dehydrated, cleared, and mounted with a coverslip. For detection of GFP^+ MSC-derived cells, explanted ossicles were fixed in 2% PFA at 4 °C overnight, then decalcified (Decal Solution, American Mastertech, Lodi, CA) for 2 – 8 hours. Specimens were processed for embedding in OCT by cryoprotection in sucrose and sectioned on a cryotome. Representative sections were counter-stained with DAPI and thereafter a standard hematoxylin and eosin staining was performed. All images were captured using a Leica DM5500 microscope and Leica Application Suite V4 software.

Lentiviral production

HEK293TN cells (System Biosciences, Mountain View, CA) were grown in DMEM high glucose medium (Hyclone, GE Healthcare Life Sciences, Pittsburgh, PA)) supplemented with 10% FBS, 2 mM L-Glutamine, 25mM Hepes, and 1× non-essential amino acids (NEAA, Thermo). 24 hours before transfection, $8 – 9 \times 10^6$ cells were plated in a 150 mm tissue-culture dish. For transfection, 13.5 μg of the GIPZ lentiviral shRNA plasmid expressing a scrambled RNA control was combined with 8.8 μg of the packaging vector psPAX2 and 4.7 μg of the envelope expressing plasmid pCMV-VSV-G. The DNA mixture was diluted in Opti-MEM I medium (Thermo Fisher) and admixed with 293fectin transfection reagent (Thermo Fisher) at a ratio of 3 μl per 1 μg of DNA and thereafter dropwise added to HEK293TN cells. Viral supernatant was collected at 60 h after transfection, filtered through a 0.45 μm PVDF filter and concentrated through ultracentrifugation (Sorvall, Thermo Fisher; 23,000 rpm, 4 °C, 2 hours). The concentrated

lentiviral particles were resuspended over night in HBSS with 25 mM HEPES and stored at −80 °C.

Lentiviral transduction

Early passage BM-MSC were cultured in 10 cm dishes to 70 – 80% confluence in alpha-MEM supplemented with 10% pHPL. For transduction alpha MEM was removed, cells were washed twice with pre-warmed PBS and lentiviral particles were added in 5 mL OptiMEM I medium supplemented with 2% FBS and 50 μg/mL protamine sulfate (Sigma). Lentiviral particles were removed after 8 hours and cells were changed back to standard alpha MEM 10% pHPL. After 2 days of recovery, transduced cells were selected by adding 5 μg/ml puromycin for 48 hours. GFP^+ cells were passaged and further expanded to reach quantities sufficient for transplantation for humanized ossicle niche formation.

Absolute quantification of engrafted leukemia cells

The total number of $mCD45.1^+$ nucleated cells recoverable per humanized ossicle-niche or mouse femur was quantified using Countbright absolute counting beads (Thermo Fisher) on a FACS Canto II flow cytometer (BD). The absolute number of total mouse BM cells was extrapolated as previously described.[55] To calculate total human leukemia cells engrafted within the total humanized ossicle-niche space as compared to the mouse BM, the percentage of human $CD45^+CD33^+$ (determined by flow-cytometry) was multiplied with the maximal number of cells recoverable from all the humanized ossicle-niche space (4 ossicles combined) or the corresponding total mouse BM. (e.g. average TNC in 4 ossicles: 5.83×10^7, $5.83 \times 10^7 \times 98.4\%$ [engraftment%] = 5.74×10^7 human leukemia cells.

Statistics

P values were calculated using non-parametric two-tailed Mann-Whitney test or unpaired student's t-test in Prism version 6 (GraphPad Software, Inc. La Jolla, CA). A *P* value less than 0.05 was considered statistically significant. Limiting-dilution data are presented as the estimated limiting dilution frequency ± 95% confidence interval. Limiting-dilution analysis was done with the Extreme Limiting Dilution Analysis (ELDA) software provided by the Walter and Eliza Hall Institute of Medical Research Bioinformatics.

Supplementary Material

Refer to Web version on PubMed Central for supplementary material.

Acknowledgments

We acknowledge the Hematology Division Tissue Bank and the patients for donating their samples. We acknowledge F. Zhao for lab management, N. Hofmann and B. Luo for technical assistance with ossicle analysis and Calreticulin sequencing and the Stanford Cytogenetics Lab for FISH analysis. A.R. is supported by an Erwin-Schroedinger Research Fellowship (Austrian Science Fund) and D.T. by a CJ Martin Overseas Biomedical Reserach Fellowship (NHMRC, Australia). R.M. is a New York Stem Cell Foundation Robertson Investigator. This research was supported by the New York Stem Cell Foundation and National Institutes of Health grants R01CA188055 and U01HL099999 to R.M.

References

1. Doulatov S, Notta F, Laurenti E, Dick JE. Hematopoiesis: a human perspective. Cell Stem Cell. 2012; 10:120–136. [PubMed: 22305562]
2. Wunderlich M, et al. AML xenograft efficiency is significantly improved in NOD/SCID-IL2RG mice constitutively expressing human SCF, GM-CSF and IL-3. Leukemia. 2010; 24:1785–1788. [PubMed: 20686503]
3. Nicolini FE, Cashman JD, Hogge DE, Humphries RK, Eaves CJ. NOD/SCID mice engineered to express human IL-3, GM-CSF and Steel factor constitutively mobilize engrafted human progenitors and compromise human stem cell regeneration. Leukemia. 2004; 18:341–347. [PubMed: 14628073]
4. Rongvaux A, et al. Development and function of human innate immune cells in a humanized mouse model. Nat Biotechnol. 2014; 32:364–372. [PubMed: 24633240]
5. Willinger T, et al. Human IL-3/GM-CSF knock-in mice support human alveolar macrophage development and human immune responses in the lung. Proc Natl Acad Sci U S A. 2011; 108:2390–2395. [PubMed: 21262803]
6. Goyama S, Wunderlich M, Mulloy JC. Xenograft models for normal and malignant stem cells. Blood. 2015; 125:2630–2640. [PubMed: 25762176]
7. Sarry JE, et al. Human acute myelogenous leukemia stem cells are rare and heterogeneous when assayed in NOD/SCID/IL2Rgammac-deficient mice. J Clin Invest. 2011; 121:384–395. [PubMed: 21157036]
8. Sanchez PV, et al. A robust xenotransplantation model for acute myeloid leukemia. Leukemia. 2009; 23:2109–2117. [PubMed: 19626050]
9. Patel S, et al. Successful xenografts of AML3 samples in immunodeficient NOD/shi-SCID IL2Rgamma(-)/(-) mice. Leukemia. 2012; 26:2432–2435. [PubMed: 22699451]
10. Kim D, Park CY, Medeiros BC, Weissman IL. CD19-CD45 low/- CD38 high/CD138+ plasma cells enrich for human tumorigenic myeloma cells. Leukemia. 2012; 26:2530–2537. [PubMed: 22733078]
11. Kim D, et al. Anti-CD47 antibodies promote phagocytosis and inhibit the growth of human myeloma cells. Leukemia. 2012; 26:2538–2545. [PubMed: 22648449]
12. Pang WW, et al. Hematopoietic stem cell and progenitor cell mechanisms in myelodysplastic syndromes. Proc Natl Acad Sci U S A. 2013; 110:3011–3016. [PubMed: 23388639]
13. Medyouf H, et al. Myelodysplastic Cells in Patients Reprogram Mesenchymal Stromal Cells to Establish a Transplantable Stem Cell Niche Disease Unit. Cell Stem Cell. 2014
14. Mendelson A, Frenette PS. Hematopoietic stem cell niche maintenance during homeostasis and regeneration. Nat Med. 2014; 20:833–846. [PubMed: 25100529]
15. Ishikawa F, et al. Chemotherapy-resistant human AML stem cells home to and engraft within the bone-marrow endosteal region. Nat Biotechnol. 2007; 25:1315–1321. [PubMed: 17952057]
16. Schepers K, Campbell TB, Passegue E. Normal and leukemic stem cell niches: insights and therapeutic opportunities. Cell Stem Cell. 2015; 16:254–267. [PubMed: 25748932]
17. Reinisch A, et al. Epigenetic and in vivo comparison of diverse MSC sources reveals an endochondral signature for human hematopoietic niche formation. Blood. 2015; 125:249–260. [PubMed: 25406351]
18. Song J, et al. An in vivo model to study and manipulate the hematopoietic stem cell niche. Blood. 2010; 115:2592–2600. [PubMed: 20110425]
19. Pettway GJ, et al. Anabolic actions of PTH (1-34): use of a novel tissue engineering model to investigate temporal effects on bone. Bone. 2005; 36:959–970. [PubMed: 15878317]
20. Zhang J, et al. Identification of the haematopoietic stem cell niche and control of the niche size. Nature. 2003; 425:836–841. [PubMed: 14574412]
21. Klco JM, et al. Functional heterogeneity of genetically defined subclones in acute myeloid leukemia. Cancer cell. 2014; 25:379–392. [PubMed: 24613412]
22. Lapidot T, et al. A cell initiating human acute myeloid leukaemia after transplantation into SCID mice. Nature. 1994; 367:645–648. [PubMed: 7509044]

23. Bonnet D, Dick JE. Human acute myeloid leukemia is organized as a hierarchy that originates from a primitive hematopoietic cell. Nat Med. 1997; 3:730–737. [PubMed: 9212098]
24. Grimwade D, Enver T. Acute promyelocytic leukemia: where does it stem from? Leukemia. 2004; 18:375–384. [PubMed: 14737069]
25. Kralovics R, et al. A gain-of-function mutation of JAK2 in myeloproliferative disorders. N Engl J Med. 2005; 352:1779–1790. [PubMed: 15858187]
26. Baxter EJ, et al. Acquired mutation of the tyrosine kinase JAK2 in human myeloproliferative disorders. Lancet. 2005; 365:1054–1061.
27. Klampfl T, et al. Somatic mutations of calreticulin in myeloproliferative neoplasms. N Engl J Med. 2013; 369:2379–2390. [PubMed: 24325356]
28. Nangalia J, et al. Somatic CALR mutations in myeloproliferative neoplasms with nonmutated JAK2. N Engl J Med. 2013; 369:2391–2405. [PubMed: 24325359]
29. James C, et al. The hematopoietic stem cell compartment of JAK2V617F-positive myeloproliferative disorders is a reflection of disease heterogeneity. Blood. 2008; 112:2429–2438. [PubMed: 18612101]
30. Ishii T, et al. Behavior of CD34+ cells isolated from patients with polycythemia vera in NOD/SCID mice. Exp Hematol. 2007; 35:1633–1640. [PubMed: 17764815]
31. Wang X, et al. Spleens of myelofibrosis patients contain malignant hematopoietic stem cells. J Clin Invest. 2012; 122:3888–3899. [PubMed: 23023702]
32. Dameshek W. Some speculations on the myeloproliferative syndromes. Blood. 1951; 6:372–375. [PubMed: 14820991]
33. Majeti R, Park CY, Weissman IL. Identification of a hierarchy of multipotent hematopoietic progenitors in human cord blood. Cell Stem Cell. 2007; 1:635–645. [PubMed: 18371405]
34. Eppert K, et al. Stem cell gene expression programs influence clinical outcome in human leukemia. Nat Med. 2011; 17:1086–1093. [PubMed: 21873988]
35. Goardon N, et al. Coexistence of LMPP-like and GMP-like leukemia stem cells in acute myeloid leukemia. Cancer cell. 2011; 19:138–152. [PubMed: 21251617]
36. Takatsuki H, et al. PML/RAR alpha fusion gene is expressed in both granuloid/macrophage and erythroid colonies in acute promyelocytic leukaemia. Br J Haematol. 1993; 85:477–482. [PubMed: 8136268]
37. Turhan AG, et al. Highly purified primitive hematopoietic stem cells are PML-RARA negative and generate nonclonal progenitors in acute promyelocytic leukemia. Blood. 1995; 85:2154–2161. [PubMed: 7536493]
38. Haferlach T, et al. Cell lineage specific involvement in acute promyelocytic leukaemia (APL) using a combination of May-Grunwald-Giemsa staining and fluorescence in situ hybridization techniques for the detection of the translocation t(15;17)(q22;q12). Br J Haematol. 1998; 103:93–99. [PubMed: 9792295]
39. Knuutila S, et al. Cell lineage involvement of recurrent chromosomal abnormalities in hematologic neoplasms. Genes Chromosomes Cancer. 1994; 10:95–102. [PubMed: 7520272]
40. Guibal FC, et al. Identification of a myeloid committed progenitor as the cancer-initiating cell in acute promyelocytic leukemia. Blood. 2009; 114:5415–5425. [PubMed: 19797526]
41. Brown D, et al. A PMLRARalpha transgene initiates murine acute promyelocytic leukemia. Proc Natl Acad Sci U S A. 1997; 94:2551–2556. [PubMed: 9122233]
42. Grignani F, et al. PML/RAR alpha fusion protein expression in normal human hematopoietic progenitors dictates myeloid commitment and the promyelocytic phenotype. Blood. 2000; 96:1531–1537. [PubMed: 10942402]
43. Matsushita H, et al. Establishment of a humanized APL model via the transplantation of PML-RARA-transduced human common myeloid progenitors into immunodeficient mice. PLoS One. 2014; 9:e111082. [PubMed: 25369030]
44. Wang X, et al. Sequential treatment of CD34+ cells from patients with primary myelofibrosis with chromatin-modifying agents eliminate JAK2V617F-positive NOD/SCID marrow repopulating cells. Blood. 2010; 116:5972–5982. [PubMed: 20858855]

45. Rongvaux A, et al. Human thrombopoietin knockin mice efficiently support human hematopoiesis in vivo. Proc Natl Acad Sci U S A. 2011; 108:2378–2383. [PubMed: 21262827]
46. Willinger T, Rongvaux A, Strowig T, Manz MG, Flavell RA. Improving human hemato-lymphoid-system mice by cytokine knock-in gene replacement. Trends Immunol. 2011; 32:321–327. [PubMed: 21697012]
47. Groen RW, et al. Reconstructing the human hematopoietic niche in immunodeficient mice: opportunities for studying primary multiple myeloma. Blood. 2012; 120:e9–e16. [PubMed: 22653974]
48. Alvarez LL, Pardo HG. Guide for the care and use of laboratory animals - Natl-Res-Council. Psicothema. 1997; 9:232–234.
49. Rohde E, Schallmoser K, Bartmann V, Reinisch A, S D. GMP Compliant Propagation of Human Multipotent Mesenchymal Stromal Cells (MSC). The pharmaceutical development handbook. 2008
50. Schallmoser K, et al. Rapid large-scale expansion of functional mesenchymal stem cells from unmanipulated bone marrow without animal serum Tissue Eng Part C Methods. 2008; 14:185–196. [PubMed: 18620484]
51. Dominici M, et al. Minimal criteria for defining multipotent mesenchymal stromal cells. The International Society for Cellular Therapy position statement. Cytotherapy. 2006; 8:315–317. [PubMed: 16923606]
52. Notta F, et al. Isolation of single human hematopoietic stem cells capable of long-term multilineage engraftment. Science. 2011; 333:218–221. [PubMed: 21737740]
53. Moraga I, et al. Tuning cytokine receptor signaling by re-orienting dimer geometry with surrogate ligands. Cell. 2015; 160:1196–1208. [PubMed: 25728669]
54. Corces-Zimmerman MR, Hong WJ, Weissman IL, Medeiros BC, Majeti R. Preleukemic mutations in human acute myeloid leukemia affect epigenetic regulators and persist in remission. Proc Natl Acad Sci U S A. 2014; 111:2548–2553. [PubMed: 24550281]
55. Boggs DR. The total marrow mass of the mouse: a simplified method of measurement. American journal of hematology. 1984; 16:277–286. [PubMed: 6711557]

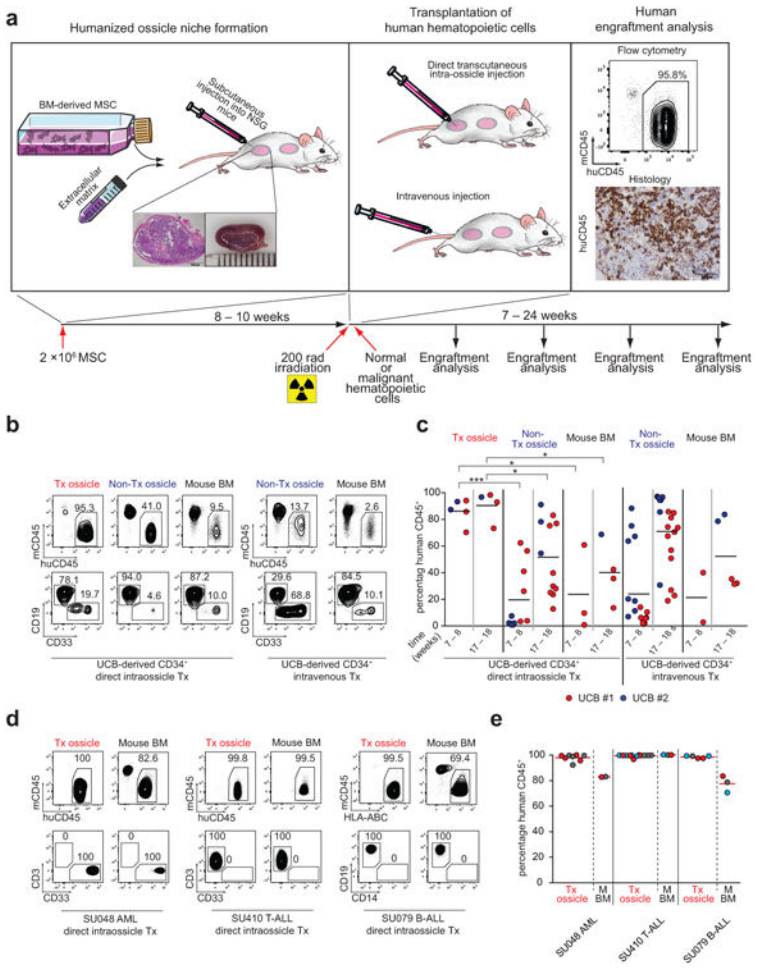

Figure 1. Human hematopoietic stem and progenitor cells and primary acute leukemia engraft robustly in human BM-MSC-derived ossicles

(**a**) Experimental schematic and time line (below). **(b,d)** Representative FACS-plots showing human normal (**b**) and leukemic (**d**) engraftment at indicated time points post-transplantation. (n = 2 – 20 per group). 1×10^4 UCB-derived $CD34^+$ hematopoietic stem and progenitor cells (HSPC), 10,000 AML blasts (SU048), 1×10^5 T-ALL blasts (SU410), and 8.3×10^5 B-ALL blasts (SU079) were transplanted either intravenously (**b**, right panel) or directly into one out of four ossicles (**b**, left panel, **d**). Transplanted (Tx ossicle), non-transplanted ossicles (Non-Tx ossicle), and mouse bone marrow (BM) were analyzed by flow cytometry for the presence of human normal or leukemic $CD45^+$ cells. Engrafted normal cells were further gated for myeloid cells ($CD45^+CD33^+$) and B lymphoid cells ($CD45^+CD19^+$). Leukemia engraftment was confirmed by exclusive expression of CD33 (SU048, AML), CD3 (SU410, T-ALL) and CD19 (SU079, B-ALL). (**c,e**) Summary of human chimerism levels in ossicles and mouse BM. For (**c**): Dots represent individual engrafted ossicles at the indicated time points post-transplantation. (Tx ossicle after direct intraossicle Tx: 7 – 8 weeks, n = 5; 17 – 18 weeks, n = 4; Non-Tx ossicle after direct intraossicle Tx: 7 – 8 weeks, n = 13; 17 – 18 weeks, n = 12; mouse BM after direct intraossicle Tx: 7 – 8 weeks, n = 3; 17 – 18 weeks, n = 4; Tx ossicle after intravenous Tx: 7 – 8 weeks, n = 19; 17 – 18 weeks, n = 20; mouse BM after direct intraossicle Tx: 7 – 8

weeks, $n = 2$; 17 – 18 weeks, $n = 5$). * $P < 0.05$; *** $P < 0.001$, Mann-Whitney U test. All analyzed tissues were included in the analysis. Differences in numbers are due to technical failure in some ossicle aspirates. For (**e**): Each dot represents one separately transplanted ossicle (AML, $n = 8$; T-ALL, $n = 12$; B-ALL, $n = 5$) or mouse (AML, $n = 2$; T-ALL, $n = 3$; B-ALL, $n = 3$). Lines represent mean engraftment levels, colors represent different mice.

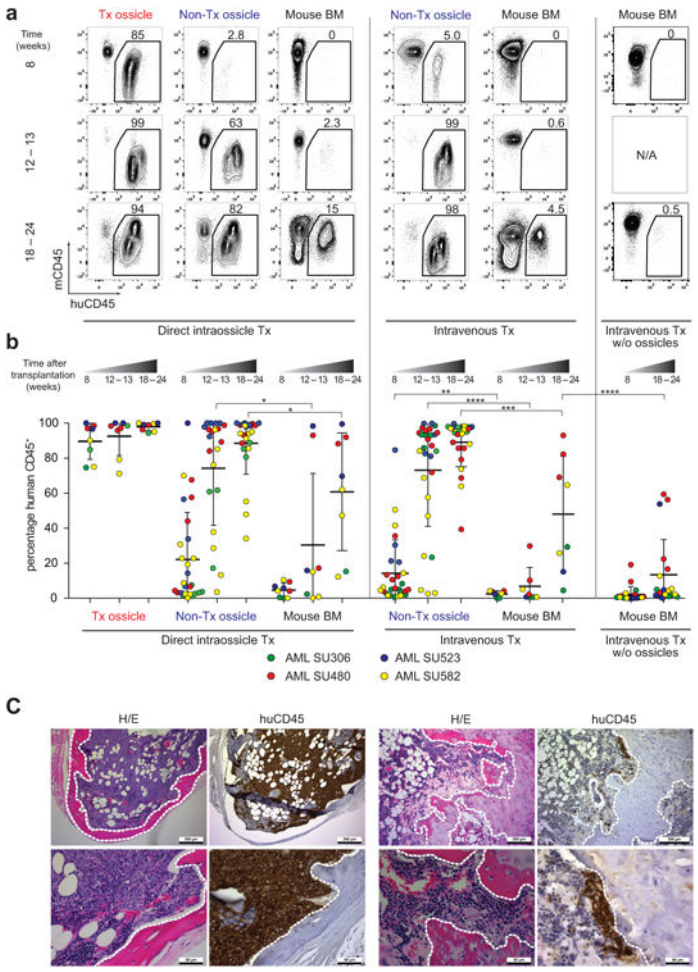

Figure 2. Primary AML blasts preferentially engraft humanized ossicle niches compared to mouse bone marrow

(**a**) Representative FACS plots of human leukemia engraftment at 8, 12 – 13, and 18 – 24 weeks post transplantation. 1×10^6 T cell-depleted MNCs were transplanted (i) directly into one out of four humanized ossicle niches per mouse (direct intraossicle Tx), (ii) intravenously into mice bearing four ossicles, or (iii) intravenously into mice without ossicles (left to right). Transplanted (Tx ossicle) and non-transplanted ossicles (Non-Tx ossicle), as wells as mouse bone marrow (BM) were analyzed for the presence of human $CD45^+CD33^+$ AML cells. (n = 7 – 28 per group). (**b**) Summary of human leukemia engraftment over time in the ossicles and mouse BM. Each dot represents one ossicle or mouse BM. Black lines represent mean engraftment ± SD. Four different primary AML samples are color coded as indicated. (Tx ossicle after direct intraossicle Tx: 8 weeks, $n = 8$; 12 – 13 weeks, $n = 8$; 18 – 24 weeks, $n = 8$; Non-Tx ossicles after direct intraossicle Tx: 8 weeks, $n = 27$; 12 – 13 weeks, $n = 22$; 18 – 24 weeks, $n = 24$; mouse BM after direct intraossicle Tx: 8 weeks, $n = 9$; 12 – 13 weeks, $n = 9$; 18 – 24 weeks, $n = 8$; Non-Tx ossicles after intravenous Tx: 8 weeks, $n = 28$; 12 – 13 weeks, $n = 28$; 18 – 24 weeks, $n = 28$; mouse BM after intravenous Tx: 8 weeks, $n = 7$; 12 – 13 weeks, $n = 7$; 18 – 24 weeks, $n = 7$; mouse BM after intravenous Tx without ossicles: 8 weeks, $n = 12$; 18 – 24 weeks, $n = 12$) * $P < 0.05$; ** $P < 0.01$; *** $P < 0.001$; **** $P < 0.0001$, Mann-Whitney U test. (**c**) Representative

histological analysis of explanted Tx ossicles (left panel) and Non-Tx ossicles (right panel) eight weeks post-transplantation. At least two engrafted ossicles were analyzed per primary AML sample SU306, SU480, SU532 and SU582. Hematoxylin/Eosin (H/E) and immunostaining for human CD45 are shown in low (upper panels) and high (lower panels) magnification. Scale bars, 200 μm and 50 μm. White dotted lines indicate endosteal bone surface. N/A: not analyzed.

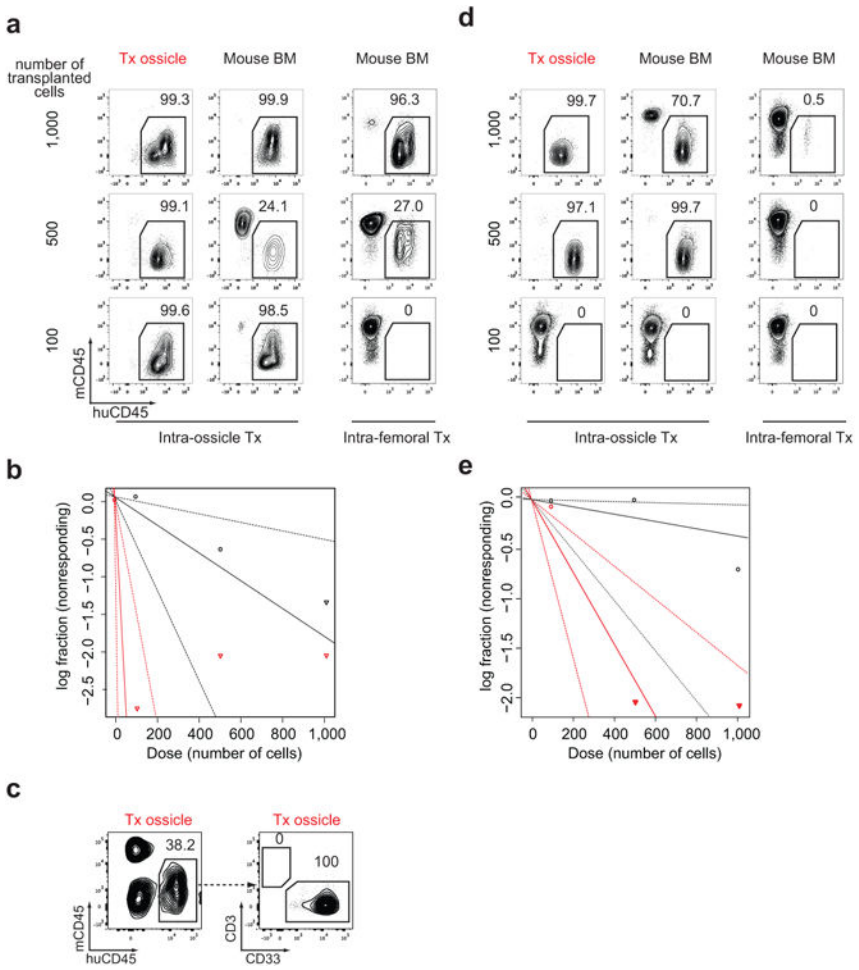

Figure 3. Humanized ossicle niche transplantation reveals an increased leukemia-initiating cell frequency in AML

NSG mice were transplanted directly into humanized ossicle niches (intraossicle Tx) or intrafemorally with varying numbers (1,000; 500; 100 or 1) of T cell-depleted MNC from AML samples SU028 (**a**) and SU048 (**d**) and analyzed for engraftment 14 weeks post-transplantation by flow cytometry. Representative FACS plots (n = 2-24 per group) showing human leukemia engraftment in the ossicles (Tx ossicle) and mouse bone marrow (BM) are indicated. (**b,e**) The frequency of leukemia-initiating cells was determined by limiting dilution analysis as described in the methods. (**c**) Engraftment analysis from direct intraossicle transplantation of a single $CD34^+CD38^-$ cell from case SU028 by monitoring of human $CD45^+CD33^+$ cells in the transplanted ossicle.

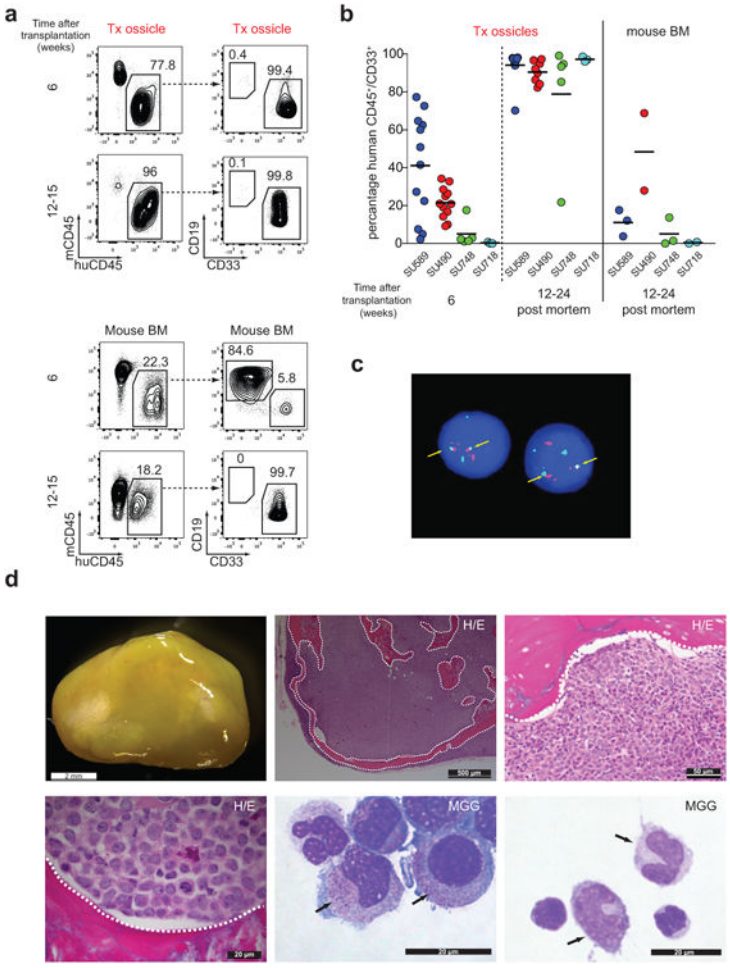

Figure 4. Humanized ossicle niches facilitate robust engraftment of acute promyelocytic leukemia cells which likely derive from lineage-committed leukemia-initiating cells

(**a**) Representative FACS analysis from engrafted primary APL sample SU589 showing human $CD45^+$ cells at 6 and 12 – 15 weeks post-transplantation of 1×10^6 primary T cell-depleted MNC. ($n = 2 – 12$ per group). Cells were directly transplanted into humanized ossicle niches, and transplanted ossicles (Tx ossicle, upper panel), as well as mouse bone marrow (BM, lower panel) were analyzed for the presence of human $CD45^+CD33^+$ myeloid and $CD45^+CD19^+$ lymphoid cells. (**b**) Summary of human APL engraftment over time. Each dot represents one transplanted ossicle. Individual APL samples SU589, SU490, SU748, and SU718 are color-coded. Lines represent mean engraftment. (for Tx ossicles: SU589 6 weeks, $n = 12$; SU490 6 weeks, $n = 12$; SU748 6 weeks, $n = 5$; SU718 6 weeks $n = 3$; SU589 12 – 24 weeks, $n = 12$; SU490 12 – 24 weeks, $n = 12$; SU748 12 – 24 weeks, $n = 5$; SU718 12 – 24 weeks $n = 3$; for mouse BM: SU589 12 – 24 weeks, $n = 3$; SU490 12 – 24 weeks, $n = 3$; SU748 12 – 24 weeks, $n = 3$; SU718 12 – 24 weeks $n = 2$) (**c**) Interphase fluorescence in situ hybridization (FISH) for PML-RARA translocation on sorted human $CD45^+CD33^+$ blasts from humanized ossicle niches engrafted with primary APL sample SU589. Engrafted APL blasts were FACS-purified as human $CD45^+CD33^+$ cells. Yellow arrows mark chromosomal fusion events indicative for t(15;17). Magnification: 100× objective (**d**) Macroscopic image (top left) of APL engrafted, explanted humanized ossicle.

Yellowish/greenish hue reflects massive engraftment of human APL cells. Scale bar represents 2 mm. Histological analysis of explanted engrafted ossicles (H/E, top middle, top right, bottom left) and morphological analysis of engrafted cells on May-Gruenwald-Giemsa (MGG) stained cytospins (bottom middle and bottom right). White dashed lines mark the endosteal surface. Black arrows mark azurophilic granules (bottom middle) and pathognomonic, bi-lobed, cerebriform APL blasts (bottom right). Scale bar: 500, 20, 50, and 20 μm (left to right).

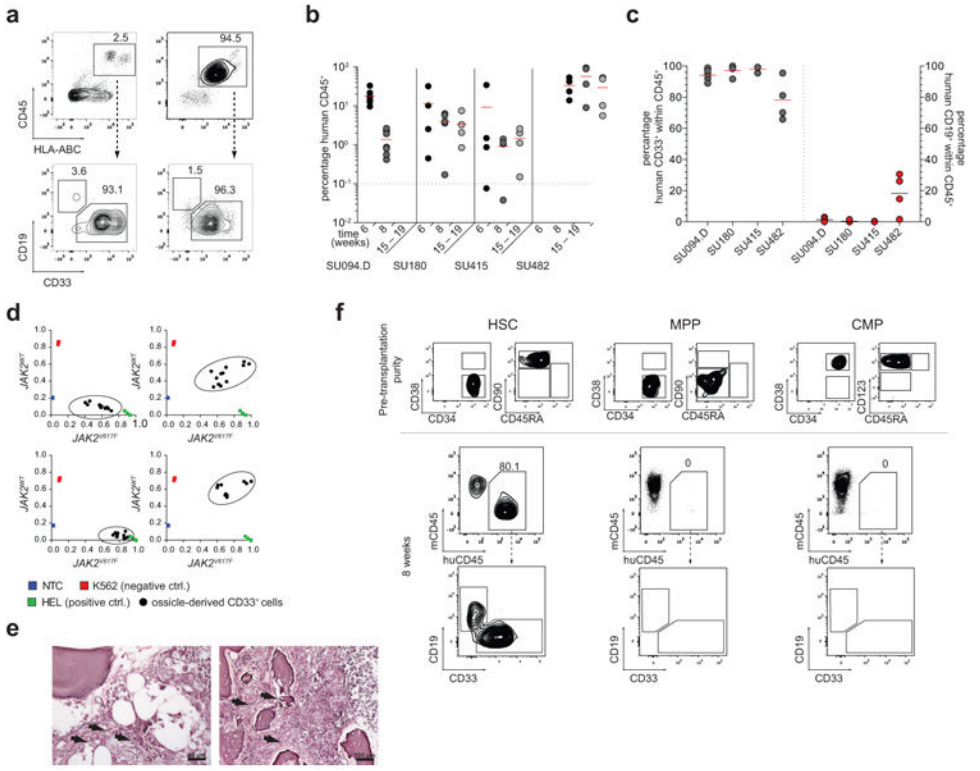

Figure 5. Humanized ossicle niches facilitate robust engraftment of myelofibrosis which derives from leukemia-initiating cells in the HSC compartment

(**a**) Representative FACS plots showing engraftment eight weeks after direct intraossicle transplantation of FACS-purified $CD34^{+}CD38^{-}$ cells from MF samples SU094.D (left panel) and SU482 (right panel). ($n = 4 – 7$ per sample) (**b,c**) Summary of human $CD45^{+}$ engraftment kinetics (**b**) and (**c**) percentage of $CD33^{+}$ myeloid cells (grey dots) versus $CD19^{+}$ B cells (red dots) among engrafted human $CD45^{+}$ cells at six weeks post transplantation of MF samples SU094, SU180, SU415 and SU482. Each dot represents one transplanted ossicle and horizontal lines indicate mean engraftment levels. (SU094.D, $n = 7$; SU180, $n = 4$; SU415.D, $n = 4$; SU482, $n = 4$) (**d**) *JAK2* mutation status of engrafted $CD33^{+}$ myeloid cells tested from MF samples SU094.D, SU180 (top panels), SU451 and SU482 (lower panels) by custom Taqman single nucleotide polymorphism (SNP) genotyping assays. Cells isolated from ossicles (black circles) were either classified as wild type (WT) ($JAK2^{WT}$, y-axis) or mutated ($JAK2^{V617F}$, x-axis) based on comparison with cell lines know to be either WT (K562, red rectangles) or mutated (HEL, green rectangles), or no template control (NTC, blue rectangles). Reactions were performed in triplicate. (**e**) Reticulin stain of explanted ossicles engrafted with MF sample SU180. Black arrows indicate presence of reticulin fibers. Scale bar represents 50 μm and 100 μm as indicated. (**f**) FACS plots depicting pre-transplantation purity (upper panel) of FACS-purified HSC, MPP, and CMP isolated from MF sample SU482 and the percentage of human $CD45^{+}$ engraftment within transplanted ossicles 8 weeks post-transplantation (lower panel) further gated for myeloid cells ($CD45^{+}CD33^{+}$) and B lymphoid cells ($CD45^{+}CD19^{+}$).

Table 1

Summary of engraftment assays of primary transplanted AML samples

Sample ID	Specimen type	WHO classification	No. of transplanted cells	Engraftment in ossicles (io Tx) (mean ± SD, time after Tx)	Engraftment in ossicles (iv Tx) (mean ± SD, time after Tx)	Engraftment iv Tx (no ossicles) (mean ± SD, time after Tx) No. of transplanted cells
SU306	pB	AML NOS	1×10^6 MNC (T-cell depleted)	97.6 ± 1.5 (24 weeks)	96.9 ± 1.6 (24 weeks)	2.1. ± 1.9 (18 weeks) 1×10^6 MNC (T-cell depleted)
SU480	pB	AML NOS	0.9×10^6 MNC (T-cell depleted)	97.8 ± 2.3 (22 weeks)	80.1 ± 18.5 (22 weeks)	31.6 ± 25.0 (18 weeks) 1×10^6 MNC (T-cell depleted)
SU532	pB	AML NOS	1×10^6 MNC T-cell depleted)	99.5 ± 0.7 (18 weeks)	98.4 ± 1.1 (18 weeks)	12.2 ± 23.3 (18 weeks) 1×10^6 MNC (T-cell depleted)
SU582	pB	AML NOS	1×10^6 MNC (T-cell depleted)	98.1 ± 2.6 (18 weeks)	88.8 ± 12.8 (18 weeks)	5.4 ± 4.3 (18 weeks) 1×10^6 MNC (T-cell depleted)
SU490	pB	APL with PML/RARA	1×10^6 MNC (T-cell depleted)	97.4 ± 1.9 (15 weeks)	n.d.	2.2 ± 1.8 (18 weeks) 1×10^6 MNC (T-cell depleted)
SU589	pB	APL with PML/RARA	1.4×10^6 MNC (T-cell depleted)	94.6 ± 8.2 (14 weeks)	n.d.	5.8 ± 4.9 (18 weeks) 1.4×10^6 MNC (T-cell depleted)
SU718	BM	APL with PML/RARA	1×10^6 MNC (FACS sorted blasts)	97.2 ± 1.3 (24 weeks)	n.d.	n.d.
SU748	pB	APL with PML/RARA	0.9×10^6 MNC (FACS sorted blasts)	78.9 ± 32.3 (24 weeks)	n.d.	n.d.
SU380	pB	AML with inv(16)(p13;q22) or t(16;16)(p13;q22)	0.8×10^6 $CD45^{dim}$ FACS-sorted blasts	98.1 ± 0.7 (16 weeks)	n.d.	6.2 ± 3.3 (18 weeks) 1×10^6 MNC (T-cell depleted)
SU080	BM	AML with inv(16)(p13;q22) or t(16;16)(p13;q22)	0.5×10^6 $CD45^{dim}$ FACS-sorted blasts	95.7 ± 2.2 (8 weeks)	n.d.	No engraftment (11 weeks) 0.5×10^6 $CD34^+$ blasts (T-cell depleted)
SU430	pB	BAL	0.75×10^6 MNC (T-cell depleted)	98.5 ± 2.4 (17 weeks)	n.d.	93.8 ± 7.2 (16 weeks) 1×10^6 MNC (T-cell depleted)
SU028	Leuk	AML NOS	100 MNC (T-cell depleted)	98.6 ± 1.8 (14 weeks)	n.d.	94.8 ± 2.9 (25 weeks) 5×10^6 MNC (T-cell depleted)
SU048	Leuk	AML NOS	1000 MNC (T-cell depleted)	97.6 ± 3.6 (14 weeks)	n.d.	98.1 ± 1.1 (12-15 weeks) 5×10^6 MNC (T-cell depleted)
SU507	pB	BAL	1×10^6 MNC (T-cell depleted)	Normal engraftment	n.d.	<1% normal engraftment (18 weeks) 1×10^6 MNC (T-cell depleted)
SU421	pB	AML with t(8;21)(q22;q22)	0.13×10^6 $CD45^{dim}$ FACS-sorted blasts	No engraftment (13 weeks)	No engraftment (18 weeks)	n.d.

Abbreviations: pB: peripheral blood; BM: bone marrow; NOS: not otherwise specified; BAL: Biphenotypic acute leukemia; MNC: mononuclear cells; Leuk: leukapheresis; BM: bone marrow; i.o. intraossicle; i.v. intravenous; n.d.: not determined, normal engraftment is defined as multi-lineage engraftment mainly consisting of B-cells with minor percentages of myeloid cells.